

Speech-Based Human-Exoskeleton Interaction for Lower Limb Motion Planning

Eddie Guo^{1,2}, Christopher Perlette³, Mojtaba Sharifi^{1,4,5}, Lukas Grasse³, Matthew Tata³, Vivian K. Mushahwar⁵, and Mahdi Tavakoli^{1,4,5}

¹Department of Electrical and Computer Engineering, University of Alberta,

²Cumming School of Medicine, University of Calgary

³Department of Neuroscience, University of Lethbridge

⁴Department of Mechanical Engineering, San Jose State University

⁵Sensory Motor Adaptive Rehabilitation Technology (SMART) Network, University of Alberta

October 6, 2023

Abstract

This study presents a speech-based motion planning strategy (SBMP) developed for lower limb exoskeletons to facilitate safe and compliant human-robot interaction. A speech processing system, finite state machine, and central pattern generator are the building blocks of the proposed strategy for online planning of the exoskeleton's trajectory. According to experimental evaluations, this speech-processing system achieved low levels of word and intent errors. Regarding locomotion, the completion time for users with voice commands was 54% faster than that using a mobile app interface. With the proposed SBMP, users are able to maintain their postural stability with both hands-free. This supports its use as an effective motion planning method for the assistance and rehabilitation of individuals with lower-limb impairments.

Keywords: Human-robot interaction, speech processing, finite state machine, central pattern generator, lower limb exoskeleton

1 Introduction

Assistive robotic systems can enhance the quality of life of people affected by neurological impairments [1]. These systems include lower limb exoskeletons, such as ReWalk [2], Indego [3], HAL [4], and Exo-H3 (used in these experiments) [5], which are designed to rehabilitate individuals with neurological impairments. In comparison with traditional physical therapies, wearable exoskeletons allow users to interact more easily with their environment, improving mobility and independence in non-ambulatory individuals [1].

To facilitate safe and compliant human-robot interactions (HRIs), the exoskeleton motion planning strategy should be intuitive and efficient to use [6]. Social HRI, where humans use body language, gestures, and speech to interact with robots, shows promise in addressing issues with physical interactions through quick and efficient identification of user intentions [7].

Although speech recognition (SR) is increasingly adopted for HRI, this adoption is generally limited to humanoid robots [7, 8]. Nonetheless, the integration of SR into other forms of robotics may improve their ergonomics and practicality for human use. For example, SR reduces the need for conventional interaction methods such as button-based interfaces or mobile apps, allowing for hands-free use of an exoskeleton. This aspect of SR benefits users who require their hands to grasp stability aids, such as crutches or a walker. Furthermore, it increases safety in emergencies, where users may find voice commands more intuitive than a tactile controller. However, these interactions are only effective if the robot can perceive what a user is saying.

Computational SR is a complex task that requires turning auditory information into text. Over the last 40 years, there have been several breakthroughs that have advanced the technology to the point where it can effectively analyze speech and produce an accurate response even under adverse conditions [9]. In particular, a neural network architecture known as the time delay neural network factorization model has been shown to be effective at acoustic modeling and speech perception [10, 11].

Natural language understanding (NLU) addresses the problem of interpreting user intentions through two primary methods. The first method (true NLU) uses a combination of keyword analysis, semantic processing, discourse processing, and context analysis to determine the meaning and intent of speech [12]. However, this strategy is not always practical because it is computationally intensive. The other primary method of intent determination involves creating a series of phrases mapped to predetermined intents. This second method (phrase mapping) is less complex and requires fewer computational resources to execute than true NLU, making it suitable for real-time intent determination. Once an NLU system has determined the user’s intent, it becomes possible to translate high-level commands into a sequence of actions that can be performed by a platform.

With high-level speech commands as an input, control systems should translate wearer intents into low-level controllers, such as position, force, or impedance controllers, to synchronize gait planning in a smooth and time-continuous manner. Furthermore, high-level commands should be subject to safety constraints to avoid sudden movements, which may lead to injuries. Finite state machines (FSMs) address this motion planning problem by acting as a central planner for transitions between exoskeleton states, such as standing and walking [13]. Thus, FSMs may serve as an interface to translate high-level user intents into motion plans for low-level controllers.

One bioinspired strategy for exoskeleton control is the central pattern generator (CPG). The CPG consists of connected nodes that can generate rhythmic patterns without receiving rhythmic inputs, facilitating joint motion synchronization necessary to recapitulate rhythmic motor behaviours such as bipedal locomotion [14, 15]. CPGs typically include parameters that allow for modulation of locomotion, which provides additional control and flexibility for the wearer [16, 17]. The ability of CPGs to generate time-continuous rhythmic motions makes them an appropriate candidate for shaping the trajectories of lower limb exoskeletons, and they have been investigated in previous studies where joint synchronization was achieved through systems of coupled differential equations [18, 19, 20, 21, 22].

In this study, a speech-based locomotion planning strategy combined social HRI, FSM, and CPG for the intelligent motion planning of a lower limb exoskeleton for bipedal locomotion. As opposed to a button-based interface, voice input was used as the primary mode of determining user intent, allowing hands-free use of an exoskeleton. These high-level commands were processed by an FSM to ensure safe and natural state transitions before being executed in low-level position controllers. The major contributions of the proposed control scheme can be summarized as follows:

- Integration of SR and a lower limb exoskeleton to create a system that allows a user’s hands to be free to use mobility aids while still controlling the exoskeleton.
- The SR system used a combination of denoising, speech perception, and NLU modules to perform SR. By using gated recurrent units for denoising alongside probabilistic phrase mapping for NLU, we achieved an accurate SR system capable of running on a low-power device in real-time without requiring a remote machine to perform computation. This allows for a self-contained SR platform that can move with a user, allowing for a broader application of speech-based controls.
- A novel set of CPG dynamics was proposed to synchronize time-continuous transitions between exoskeleton locomotion states (e.g., sit, stand, walk) in response to discrete user inputs. Speech inputs were processed through an FSM alongside joint angles and velocities to streamline state transitions (e.g., speed up, slow down). Although voice-activated robotic systems have previously been investigated [23, 24], previous CPG dynamics have not incorporated speech-based inputs for lower limb exoskeletons [14].

The proposed three-stage motion planning scheme is outlined as follows: The speech processing system is presented in Sec. 2, the CPG and motion planning strategy is presented in Sec. 3, the experimental evaluations of the proposed motion planning strategy are presented and discussed in Sec. 4, and the concluding remarks are provided in Sec. ??.

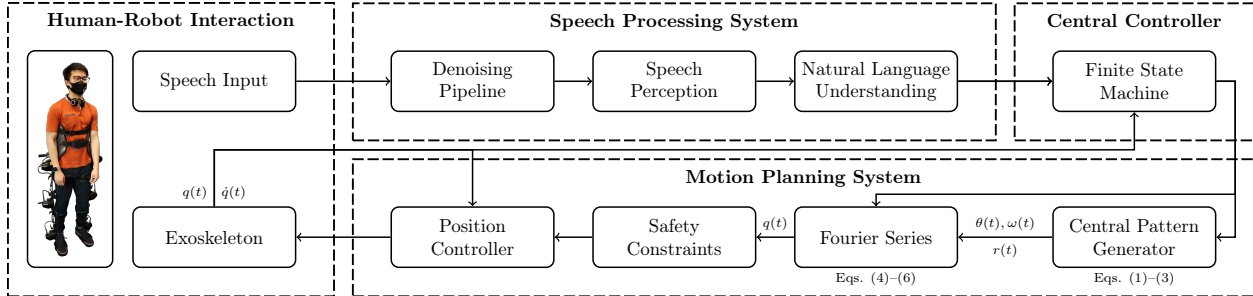


Figure 1: Proposed strategy for speech-based planning of lower limb exoskeletons.

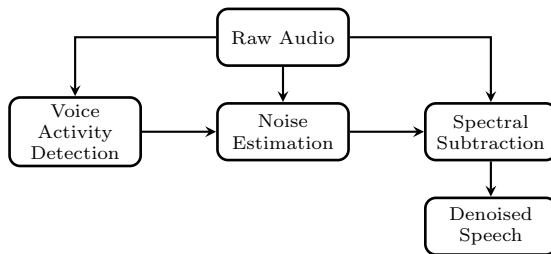


Figure 2: Major functions for denoising voice activity.

2 Speech Processing System

The proposed speech processing system was a customized version of the pipeline (Fig. 1) developed by Reverb Robotics [25], consisting of a denoising function to increase the signal-to-noise ratio (SNR), a speech perception module to process raw speech data, and a natural language understanding model to determine speech intent. Importantly, the system was able to run on a Raspberry Pi, which allowed for increased portability and for it to be applied to mobile platforms. Once an intent was determined, the Pi sent the command over a network to the central exoskeleton motion planner as shown in Fig. 1. The overall system takes approximately 0.5 seconds process and send the command to the exoskeleton control system. When factoring in network latency this results in a 500-1000 ms delay between a command being spoken and actuation of the exoskeleton.

2.1 Denoising Pipeline

The denoising function processed raw user inputs before passing the denoised signal to the speech perception function, increasing the SNR with the intention of improving the accuracy of the speech perception module in noisy environments. Denoising was achieved by detecting voice activity, analyzing its spectral signature to estimate noise, and subtracting its spectral signature of the noise from the input audio to produce the denoised audio (Fig. 2). We used RNNoise, a deep recurrent neural network, to denoise the input audio for the SR system along with embeddings provided by the developers trained on 140 hours of data. RNNoise used gated recurrent units to track long-term patterns that were difficult to process with conventional recurrent units [26]. For example, the denoising function detected fan noise and subtracted that sound from speech. Moreover, when a user moved to a different area without that noise, the function stopped removing that spectral signature and adapted to remove any new noise.

Gated recurrent units function similarly to normal long-short term memory recurrent units with the addition of two sigmoid-activated gates. These activation gates control when the recurrent unit learns and forgets information, addressing the vanishing gradient problem with classical recurrent neural networks [27]. This feature of gated recurrent units allowed the denoising function to remove persistent background noise from an input signal while preserving speech information.

Table 1: CPG parameters, initial conditions, and constants for the proposed motion planning scheme. For parameters and initial conditions, l and r refer to the left and right side of the exoskeleton, respectively.

Parameters	Initial conditions	Constants
$v_{ij} = 0.1$	$A_0(k) = 1$	$c_r = 2.5$
$\phi_{ll} = 0 \text{ rad}$	$\Omega_0(k) = \pi/2 \text{ rad}$	$c_\theta = 2 \text{ rad}$
$\phi_{rr} = 0 \text{ rad}$	$\theta_l(0) = (2 + \pi) \text{ rad}$	$\beta_\omega = 10\pi$
$\phi_{lr} = \pi \text{ rad}$	$\theta_r(0) = 2 \text{ rad}$	$\beta_r = 10\pi$
		$T = 2 \text{ s}$

2.2 Speech Perception Network

The speech processing system uses an implementation of the Vosk speech perception system [28] to perceive speech and form words. The Vosk implementation combines the time delay neural network factorization model and a multi-stream convolutional neural network. When the time delay neural network factorization architecture is combined with a multi-stream convolutional neural network architecture that allowed for simultaneous processing of several temporal windows, the result was a robust speech perception model. We used a pre-trained set of open-source weights called ‘vosk-model-small-en’ provided by Alpha Cephei [29]. Additionally, we used a constrained vocabulary to reduce the search space for SR and improve the recognition of words in the vocabulary. This is implemented by simply creating a list of words the network can perceive.

2.3 Natural Language Understanding

To address the problem of intent determination, the SR system used Snips NLU [30] to create a list of intents along with phrases that trigger those intents. Although a variety of phrases were associated with each intent, rather than using exact phrase checking, the intent parser used a probabilistic engine that focuses on keyword analysis, enabling the NLU engine to associate perceived speech with the proper intent without that speech being in the phrase list. Once an intent was extracted, the program determined whether the speech was directed at the exoskeleton. We checked if the command contained the word ‘robot’ to prevent the exoskeleton from performing an unintended action. Thus, the specific key words or phrases to trigger a state transition was ‘robot {keep moving, don’t change, maintain speed, stand up, stand, sit down, sit, stop moving, stop, walk forward, walk, move forward, move, forward, slow down, slow, speed up, go faster, faster},’ where one of the key words or phrases in the set are used (Fig. 3).

3 Motion Planning and Control

3.1 Overview of the Exoskeleton Motion Planning System

The proposed exoskeleton locomotion motion planning strategy combined a speech processing system, FSM, and CPG to ensure safe time-continuous transitions between exoskeleton states (Fig. 1). Firstly, high-level voice commands were processed through the Reverb Robotics speech processing system [25]. Then, user intents were sent to the FSM of the exoskeleton. When a new intent was received, the FSM sent an input to the CPG, which fed into a Fourier series to generate joint trajectories subject to safety constraints. The period and amplitude of the trajectory could be modulated via inputs to the FSM. Then, these signals fed into position controllers, which controlled the exoskeleton. Finally, exoskeleton joint angles and velocities fed back into the FSM in a closed loop to ensure safe transitions between exoskeleton states.

3.2 Synchronization of Joint Trajectories

The proposed CPG dynamics for the phase $\theta_i(t)$ and amplitude $r(t)$ of the i th exoskeleton joint are governed by the following equations based on the Kuramoto model for the synchronization of coupled oscillators [31].

$$\begin{aligned}\dot{\theta}_i(t) &= \omega(t) + \sum_{j=1}^N v_{ij} \sin(\theta_i(t) - \theta_j(t) - \phi_{ij}) \\ \ddot{\omega}(t) &= \lambda(t)\beta_\omega \left(\frac{\beta_\omega}{4} (\Omega_n(k) - \omega(t)) - \dot{\omega}(t) \right) \\ \ddot{r}(t) &= \lambda(t)\beta_r \left(\frac{\beta_r}{4} (A_n(k) - r(t)) - \dot{r}(t) \right)\end{aligned}\quad (1)$$

where N is the number of joints, v_{ij} is the coupling strength, ϕ_{ij} is the phase offset, β_ω and β_r are fixed constants, $\Omega_n(k)$ and $A_n(k)$ are user-adjustable constants which modulate the frequency and amplitude of the system, respectively, and $\lambda(t)$ is a user-triggered ramping system which multiplies the CPG signal by a linear time-dependent gain. In particular, $\Omega_n(k)$ and $A_n(k)$ update in response to user inputs, k (Table 1).

$$\begin{aligned}\Omega_n(k) &= \begin{cases} \Omega_{n-1} + c_\theta, & k = \text{speed up} \\ \Omega_{n-1} - c_\theta, & k = \text{slow down} \\ \Omega_{n-1}, & k = \text{otherwise} \end{cases} \\ A_n(k) &= \begin{cases} A_{n-1} + c_r, & k = \text{speed up} \\ A_{n-1} - c_r, & k = \text{slow down} \\ A_{n-1}, & k = \text{otherwise} \end{cases}\end{aligned}\quad (2)$$

Here, Ω_n and A_n are the updated speed constants, Ω_{n-1} and A_{n-1} are the current speed constants, and c_θ and c_r are constants that adjust the frequency and amplitude of the dynamics in (1).

The ramping system is defined as follows:

$$\lambda(t) = \begin{cases} t/T, & \text{stand-to-walk} \\ 1 - t/T, & \text{walk-to-stop} \\ 1, & \text{walking} \\ 0, & \text{otherwise} \end{cases}\quad (3)$$

where the stand-to-walk and walk-to-stop conditions are triggered by user commands and held for a period T (Table 1).

Coupling between all joints is maintained by the same principal frequency of $\omega(t)$ and amplitude $r(t)$ to synchronize locomotion trajectories. Furthermore, the coupling expression in (1), $v_{ij} \sin(\theta_i(t) - \theta_j(t) - \phi_{ij})$, returns the exoskeleton joints to their original trajectories if the joint phases are perturbed.

The desired walking trajectory $q_{w_i}(t)$ for the joint i of the exoskeleton is defined as

$$q_{w_i}(t) = r(t) \left(a_{0_i} + \sum_{k=1}^{N_i} (a_{k_i} \cos k\theta_i(t) + b_{k_i} \sin k\theta_i(t)) \right)\quad (4)$$

where a_{k_i} and b_{k_i} are the coefficients of Fourier series with N_i terms (Table 2). The amplitude and phase of these oscillatory motions are updated in real-time by $\theta_i(t)$ and $r(t)$. Trajectories for the ankle, knee, and hip during walking were obtained from Subject 6 in the experiments of Lencioni *et al.* [32].

The sit-to-stand and stand-to-sit trajectories for the ankle, knee, and hip are obtained from the experiments of Nuzik *et al.* [33], which included motion data for 55 healthy adults (38 women, 17 men). The mean trajectory values of all subjects for each joint were used to compute the desired sit-to-stand and stand-to-sit trajectory $q_{s_i}(t)$ for the joint i of the exoskeleton.

$$q_{s_i}(t) = a_{0_i} + \sum_{k=1}^{N_i} (a_{k_i} \cos k\omega_{s_i} t + b_{k_i} \sin k\omega_{s_i} t)\quad (5)$$

Table 2: Coefficients of the Fourier series for the hip and knee from sitting, standing, and walking.*

State	Joint	a_0	a_1	a_2	a_3	a_4	a_5	a_6	b_1	b_2	b_3	b_4	b_5	b_6
Sitting/ Standing	Hip	105.40	-1.52	1.29	0.42	0.36	-0.04	-0.12	-3.86	2.92	0.24	-0.49	-0.28	0.01
	Knee	140.20	-38.30	-1.75	0.55	1.32	0.14	n/a	-29.22	8.39	4.14	0.15	-0.39	n/a
	Ankle	49.59	22.01	-1.31	0.28	-0.07	0.15	n/a	35.11	-11.48	-4.05	-0.16	0.40	n/a
Walk	Hip	40.69	23.22	-4.49	0.40	0.70	1.08	-0.27	-8.65	3.34	1.39	0.80	0.34	0.07
	Knee	25.70	-3.83	-8.54	1.91	1.09	2.05	-0.31	-19.28	17.93	3.77	1.50	0.58	-0.90
	Ankle	-0.99	5.29	-8.58	-0.48	1.69	-0.04	1.30	3.61	-5.95	5.92	-2.12	1.02	-0.72

* $R_{\text{adj}}^2 \geq 0.99$ for each trajectory.

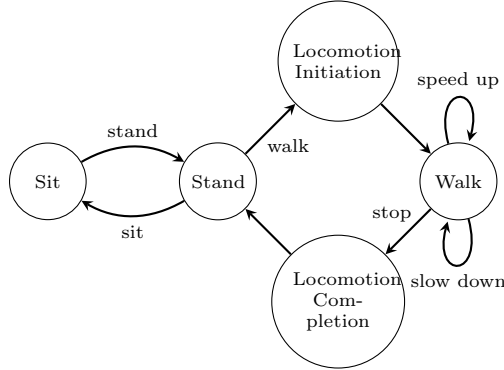


Figure 3: Proposed FSM to plan the transitions between exoskeleton states.

where ω_{s_i} is the angular frequency of the trajectory, and a_{k_i} and b_{k_i} are the coefficients of the Fourier series with N_i terms (Table 2). Equation (5) was set to satisfy the time-dependent boundary conditions $\dot{q}_{s_i}(t_0) = 0$ and $\dot{q}_{s_i}(T) = 0$, where t_0 is the initial time and T is the time after one sit-to-stand or stand-to-sit period (Table 1). The output of (5) was transformed into the coordinate system of the exoskeleton via the linear function

$$q_{t,s_i}(t) = -q_{s_i}(t) + \max(q_{s_i}(t)) \quad (6)$$

where $q_{t,s_i}(t)$ is the transformed angle. This function ensures that the endpoint for the sit-to-stand trajectory for the ankle, knee, and hip terminates at 0° . The stand-to-sit trajectory is implemented as the reverse of the sit-to-stand trajectory (i.e., $q_{t,s_i}(t) \mapsto q_{t,s_i}(-t)$ in equation 6).

3.3 Safety Considerations

The finite state machine was designed to ensure safe transitions between exoskeleton states. The states and intents for triggering transition can be seen in figure 3, and the initial state of the exoskeleton is either sitting or standing, depending on the initial position of the user. Position controller constraints include limitations on the maximum torque and velocity and maximum and minimum joint angles.

4 Experimental Evaluations

4.1 Speech Processing Experiments

Experimental assessments were performed to evaluate the efficacy of the SR system with ethics permission from the University of Lethbridge Human Subjects Review Board, number 2013-037. In the experiment, participants removed their protective mask being worn due to public health restrictions and spoke a series of pre-defined commands consistent with what would be used in normal use of the exoskeleton. After each command, the output of the SR system and NLU engine was recorded. Then, the participant put on their mask and repeated the experiment. SR performance was measured with two metrics, word error rate (WER) and intent error rate (IER). WER is a standard metric for speech perception performance that is determined

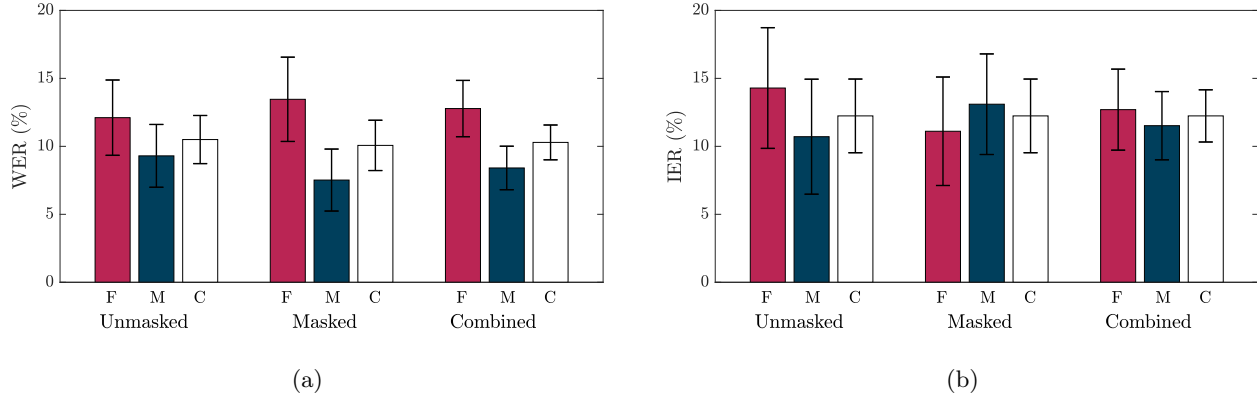


Figure 4: Results for the human SR trials for (a) WER and (b) IER. F=Female, M=Male, C=Combined. There were no significant differences between or within groups.

by the ratio of insertions (I), substitutions (S), and deletions (D) required to transform a response into the target to the number of words in the target N :

$$\text{WER} = \frac{I + S + D}{N} \times 100\% \quad (7)$$

IER is a measure of whether the correct intent was derived from the user’s speech:

$$\text{IER} = \frac{1}{N} \left(\sum_{\text{all trials}} \begin{cases} 0, & \text{correct output} \\ 1, & \text{incorrect output} \end{cases} \right) \times 100\% \quad (8)$$

This metric has a similar function to the Stanford Sentiment Treebank (SST) metric[34] that is a part of a standard NLU testing corpus General Language Understanding Evaluation[35]. SST describes the accuracy of sentiment analysis in a single sentence, though given the highly constrained nature of the model used in our project, directly using SST would not provide an accurate assessment of this model. Therefore IER was used for intent accuracy analysis. After WER and IER were calculated for individual trials, the results were aggregated to get a cumulative average for both metrics.

Experiments were performed by 4 male and 3 female participants. Participants were taken from a population of undergraduate and graduate students at the University of Lethbridge aged between 19 and 31. WER and IER scores from each participant were aggregated and computed (Fig. 4).

One drawback of the SR system has to do with the intent recognition system. By implementing a constrained vocabulary, words spoken by the user may be similar enough to words in the vocabulary where an intent might be triggered. For example, ‘hello’ may register as ‘slow’. We reduced this problem by checking for the keyword ‘robot’ before intent determination. In locomotion experiments, this feature resulted in the robot not executing commands when the word ‘robot’ was missed, particularly when a user moved into a new acoustic environment (participants moved between a quiet lab area and a room with fume hood noise) where the denoising function was not updating its model fast enough.

4.2 Locomotion Tasks With and Without Speech Commands

The proposed motion planning strategy was assessed experimentally to provide proof-of-concept evidence for the effectiveness of speech-based locomotion planning with the Exo-H3 lower limb exoskeleton from Technaid. The proposed motion planning scheme was implemented in real-time using MATLAB Simulink which received sensory data and controlled motors at a sampling rate of 100 Hz via a CAN interface (Vector VN1610) with 2 channels. The SR system was run on a Raspberry Pi 3, which received speech input from the microphone on a Logitech Wireless Headset H600 at a sampling rate of 16 000 Hz, and the processed signals were transmitted to the laptop via the user datagram protocol. The major computations in this strategy involve time integration of the CPG dynamics in equation (1) and calculating each joint angle for



Figure 5: Exo-H3 lower limb exoskeleton worn by two able-bodied users for walking. The participants use a wireless headset to command the exoskeleton. (a) User 1 (21-year-old) and (b) user 2 (33-year-old).

the exoskeleton with Fourier series in equations (4), (5), and (6). Preliminary tests were performed in a trial-and-error manner to obtain reasonable parameters for speed modulation (c_θ and c_r in equation 2) and initial values and parameters of the proposed CPG system (Table 1). In the experiments, two able-bodied users wore the exoskeleton using a walker for postural stability (Fig. 5).

The first experiment involved walking from one location, A, to another location, B, in a straight line for approximately 12m. The participants began sitting at point A, then stood and walked to point B, where they sat. Between points A and B, the user could choose to speed up or slow down ad-lib. A 21-year-old participant, user 1, and a 33-year-old participant, user 2, completed 9 and 12 trials, respectively. The time to walk in these trials for user 1 was 56 ± 2 s and that for user 2 was 66 ± 2 s ($P = 0.0023$ for a two-tailed t-test assuming equal variances, Fig. 8). The significant difference in time between users 1 and 2 to complete this experiment can be attributed to user preferences in walking speeds. The trajectory for walking from point A to point B for one representative trial of user 1 is plotted in Fig. 6 and that for user 2 is plotted in Fig. 7. These figures show the response of the exoskeleton to voice commands.

The same experiment from A to B was performed using a button-based smartphone app from Technaid with user 1 as the participant for 10 trials, and the time taken to walk from A to B was 113 ± 5 s. In comparison with the voice command time of 62 ± 2 s, a two-tailed t-test assuming equal variances yielded $P = 4.0 \times 10^{-13}$ (Fig. 8). This significant difference can be attributed to the additional time the user needed to stop the exoskeleton, remove their hands from their walker, search for the appropriate command on the exoskeleton remote control, and press that button.

5 Conclusions

In this study, a speech-based locomotion planning strategy was developed and tested to provide safe and intuitive motion planning of a lower limb exoskeleton. The proposed strategy combined a speech processing system, FSM, and CPG to plan the exoskeleton movements based on user intents. Furthermore, a novel set of speech-based CPG dynamics was developed to synchronize exoskeleton joints in a time-continuous manner in response to discrete user inputs.

To test the performance of the proposed speech processing system, WER and IER were computed as 10.29% and 12.24%, respectively, using speech data from 4 male and 3 female participants aged between 19 and 31 under both masked and unmasked conditions. The IER demonstrated is relatively low when considering limitations imposed by the hardware, as desktop computer-executed models have shown 9.6-

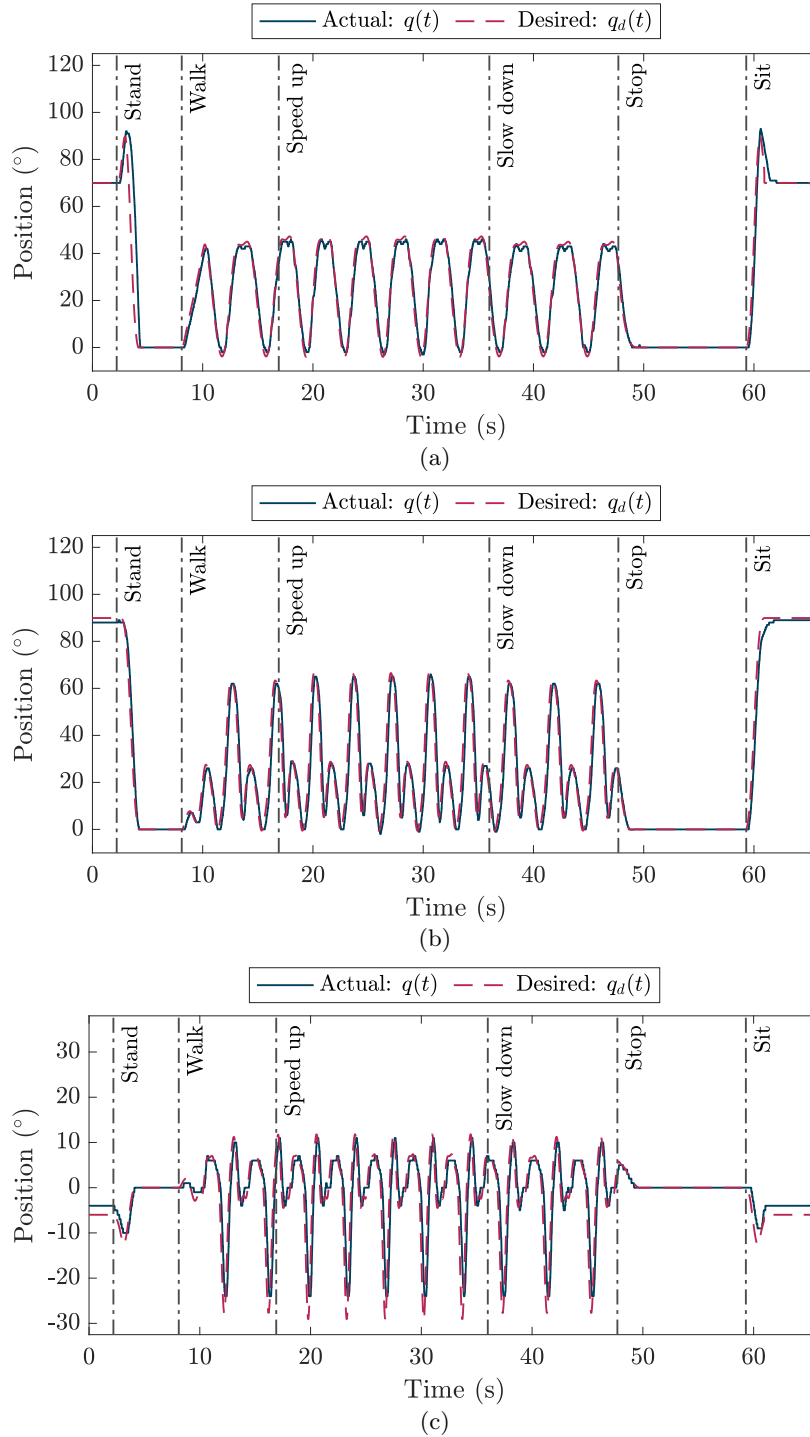


Figure 6: Actual and desired trajectories for the left (a) hip, (b) knee, and (c) ankle for the A to B locomotion task for user 1. Vertical lines correspond to the labelled speech inputs.

4.4% error rates in similar tests [36], though there is certainly room for improvement. Overall the proposed SR system could be a practical option for speech-based HRI applications when considering its performance in constrained tasks and hardware it is capable of running on.

In the user studies with the exoskeleton, voice control was compared with button control in a point-

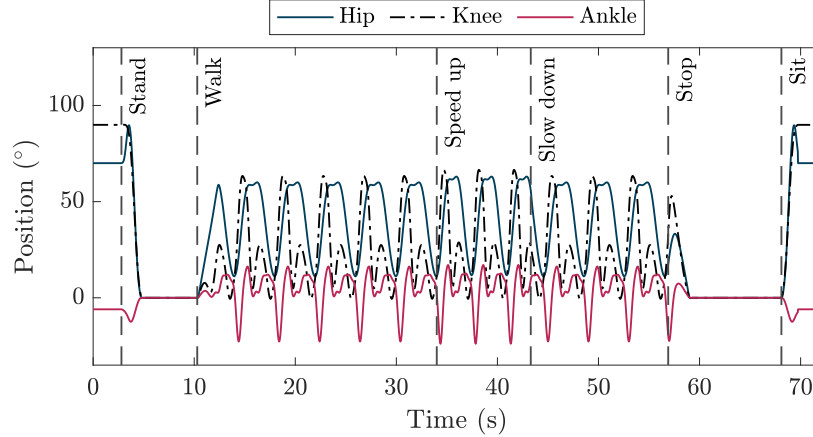


Figure 7: Desired trajectories for the left hip, knee, and ankle for the A to B locomotion task for user 2. Vertical lines correspond to the labeled speech inputs.

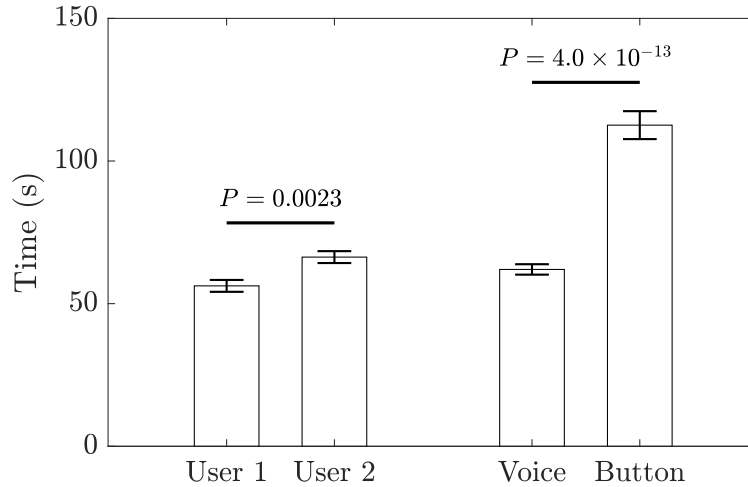


Figure 8: Time taken by users 1 and 2 to complete a locomotion task using voice control ($n_1 = 9$, $n_2 = 12$). Voice is the weighted mean time of users 1 and 2 to complete the task with voice control. Button is the mean time of user 1 to complete the task with a button-based interface ($n = 10$).

to-point locomotion task. The completion time using voice commands was 54% faster than employing a button-based mobile app interface, suggesting that voice commands may be more efficient than button-based interfaces. In addition to being efficient, speech-based planning allowed users to have both hands free to enhance postural stability and support. Thus, the combination of safety and efficiency of speech-based planning suggests it may be a promising candidate to plan the motion of lower limb exoskeletons.

5.1 Future Directions

The results of this research provide direction for future studies. First, we intend to test this system with individuals with disabilities as all participants were able-bodied. Second, we would like to improve the denoising function so it can better compensate for dynamic background noise. Finally, we want to expand the FSM and implement personalized locomotion trajectories to improve the real-world viability of the system.

CRedit Authorship Contribution Statement

Eddie Guo: Conceptualization, methodology, software, experiments, and writing. **Chris Perlette:** Methodology, software, experiments, and writing. **Mojtaba Sharifi:** Conceptualization, methodology, experiments, writing, supervision, review, and editing. **Lukas Grasse:** Software. **Matthew Tata:** Supervision, review, and editing. **Vivan K. Mushahwar:** Supervision, review, and editing. **Mahdi Tavakoli:** Supervision, review, and editing.

Declaration of Competing Interests

Authors Matthew Tata and Lukas Grasse own Reverb Robotics and developed the ReRo-Core software used as the basis for the speech recognition system.

Funding

This work was supported by the Natural Sciences and Engineering Research Council (NSERC), Canada Foundation for Innovation (CFI), Alberta Jobs, Economy and Innovation Ministry’s Major Initiatives Fund to the Center for Autonomous Systems in Strengthening Future Communities, and Autonomous Systems Initiative (ASI).

References

- [1] A. Rodríguez-Fernández, J. Lobo-Prat, and J. M. Font-Llagunes, “Systematic review on wearable lower-limb exoskeletons for gait training in neuromuscular impairments,” *Journal of NeuroEngineering and Rehabilitation*, vol. 18, 2021.
- [2] G. Zeilig, H. Weingarden, M. Zweckler, I. Dudkiewicz, A. Bloch, and A. Esquenazi, “Safety and tolerance of the rewalk™ exoskeleton suit for ambulation by people with complete spinal cord injury: A pilot study,” *The Journal of Spinal Cord Medicine*, vol. 35, no. 2, pp. 96–101, 2012.
- [3] S. A. Murray, R. J. Farris, M. Golfarb, C. Hartigan, C. Kandilakis, and D. Truex, “Fes coupled with a powered exoskeleton for cooperative muscle contribution in persons with paraplegia,” in *2018 40th Annual International Conference of the IEEE Engineering in Medicine and Biology Society (EMBC)*, 2018, pp. 2788–2792.
- [4] O. Jansen, D. Grasmuecke, R. C. Meindl, M. Tegenthoff, P. Schwenkreis, M. Sczesny-Kaiser, M. Wessling, T. A. Schildhauer, C. Fisahn, and M. Aach, “Hybrid assistive limb exoskeleton hal in the rehabilitation of chronic spinal cord injury: Proof of concept; the results in 21 patients,” *World Neurosurgery*, vol. 110, pp. e73–e78, 2018.
- [5] K. A. Inkol and J. McPhee, “Assessing control of fixed-support balance recovery in wearable lower-limb exoskeletons using multibody dynamic modelling,” in *2020 8th IEEE RAS/EMBS International Conference for Biomedical Robotics and Biomechanics (BioRob)*, 2020, pp. 54–60.
- [6] V. Villani, F. Pini, F. Leali, and C. Secchi, “Survey on human–robot collaboration in industrial settings: Safety, intuitive interfaces and applications,” *Mechatronics*, vol. 55, pp. 248–266, 2018. [Online]. Available: <https://www.sciencedirect.com/science/article/pii/S0957415818300321>
- [7] T. B. Sheridan, “Human–robot interaction: Status and challenges,” *Human Factors*, vol. 58, no. 4, pp. 525–532, 2016.
- [8] J. Kennedy, S. Lemaignan, C. Montassier, P. Lavalade, B. Irfan, F. Papadopoulos, E. Senft, and T. Belpaeme, “Child speech recognition in human-robot interaction: Evaluations and recommendations,” in *Proceedings of the 2017 ACM/IEEE International Conference on Human-Robot Interaction*, ser. HRI ’17. New York, NY, USA: Association for Computing Machinery, 2017, p. 82–90.

- [9] X. Huang, J. Baker, and R. Reddy, “A historical perspective of speech recognition,” *Commun. ACM*, vol. 57, no. 1, p. 94–103, jan 2014. [Online]. Available: <https://doi.org/10.1145/2500887>
- [10] T. F. Abidin, A. Misbullah, R. Ferdhiana, M. Z. Aksana, and L. Farsiah, “Deep neural network for automatic speech recognition from indonesian audio using several lexicon types,” in *2020 International Conference on Electrical Engineering and Informatics (ICELTICs)*, 2020, pp. 1–5.
- [11] N. Moritz, J. Schröder, S. Goetze, J. Anemüller, and B. Kollmeier, “Acoustic scene classification using time-delay neural networks and amplitude modulation filter bank features,” *complexity*, vol. 12, p. 13, 2016.
- [12] M. Bates, “Models of natural language understanding,” *Proceedings of the National Academy of Sciences*, vol. 92, no. 22, pp. 9977–9982, 1995.
- [13] K. A. Strausser and H. Kazerooni, “The development and testing of a human machine interface for a mobile medical exoskeleton,” in *2011 IEEE/RSJ International Conference on Intelligent Robots and Systems*, 2011, pp. 4911–4916.
- [14] A. J. Ijspeert, “Central pattern generators for locomotion control in animals and robots: A review,” *Neural Networks*, vol. 21, no. 4, pp. 642–653, 2008, robotics and Neuroscience.
- [15] J. Arcos-Legarda, J. Cortes-Romero, and A. Tovar, “Robust compound control of dynamic bipedal robots,” *Mechatronics*, vol. 59, pp. 154–167, 2019. [Online]. Available: <https://www.sciencedirect.com/science/article/pii/S095741581930039X>
- [16] M. Sharifi, J. K. Mehr, V. K. Mushahwar, and M. Tavakoli, “Autonomous locomotion trajectory shaping and nonlinear control for lower-limb exoskeletons,” *IEEE/ASME Transactions on Mechatronics*, vol. 27, no. 2, pp. 645–655, 2022.
- [17] S. O. Schrade, Y. Nager, A. R. Wu, R. Gassert, and A. Ijspeert, “Bio-inspired control of joint torque and knee stiffness in a robotic lower limb exoskeleton using a central pattern generator,” in *2017 International Conference on Rehabilitation Robotics (ICORR)*, 2017, pp. 1387–1394.
- [18] M. Sharifi, J. K. Mehr, V. K. Mushahwar, and M. Tavakoli, “Adaptive cpg-based gait planning with learning-based torque estimation and control for exoskeletons,” *IEEE Robotics and Automation Letters*, vol. 6, no. 4, pp. 8261–8268, 2021.
- [19] K. Gui, H. Liu, and D. Zhang, “A generalized framework to achieve coordinated admittance control for multi-joint lower limb robotic exoskeleton,” in *2017 International Conference on Rehabilitation Robotics (ICORR)*, 2017, pp. 228–233.
- [20] D. Zhang, Y. Ren, K. Gui, J. Jia, and W. Xu, “Cooperative control for a hybrid rehabilitation system combining functional electrical stimulation and robotic exoskeleton,” *Frontiers in Neuroscience*, vol. 11, p. 725, 2017.
- [21] J. K. Mehr, M. Sharifi, V. K. Mushahwar, and M. Tavakoli, “Intelligent locomotion planning with enhanced postural stability for lower-limb exoskeletons,” *IEEE Robotics and Automation Letters*, vol. 6, no. 4, pp. 7588–7595, 2021.
- [22] X. Zhang and M. Hashimoto, “Synchronization-based trajectory generation method for a robotic suit using neural oscillators for hip joint support in walking,” *Mechatronics*, vol. 22, no. 1, pp. 33–44, 2012. [Online]. Available: <https://www.sciencedirect.com/science/article/pii/S0957415811001723>
- [23] Y. Guo, W. Xu, S. Pradhan, C. Bravo, and P. Ben-Tzvi, “Personalized voice activated grasping system for a robotic exoskeleton glove,” *Mechatronics*, vol. 83, p. 102745, 2022. [Online]. Available: <https://www.sciencedirect.com/science/article/pii/S0957415822000058>
- [24] X. Wang, P. Tran, S. Callahan, S. Wolf, and J. Desai, “Towards the development of a voice-controlled exoskeleton system for restoring hand function,” 04 2019, pp. 1–7.

- [25] L. S. Grasse and M. S. Tata, “An end-to-end platform for human-robot speech interaction,” *Sound in HRI Workshop. 16th Annual Conference for Basic and Applied Human-Robot Interaction.*, Mar 2021.
- [26] J.-M. Valin, “A hybrid dsp/deep learning approach to real-time full-band speech enhancement,” 2018.
- [27] S. Hochreiter, “The vanishing gradient problem during learning recurrent neural nets and problem solutions,” *International Journal of Uncertainty, Fuzziness and Knowledge-Based Systems*, vol. 06, no. 02, pp. 107–116, 1998. [Online]. Available: <https://doi.org/10.1142/S0218488598000094>
- [28] K. J. Han, J. Pan, V. K. N. Tadala, T. Ma, and D. Povey, “Multistream cnn for robust acoustic modeling,” 2021.
- [29] “Vosk models.” [Online]. Available: <https://alphacephei.com/vosk/models>
- [30] A. Coucke, A. Saade, A. Ball, T. Bluche, A. Caulier, D. Leroy, C. Doumouro, T. Gisselbrecht, F. Caltagirone, T. Lavril, M. Primet, and J. Dureau, “Snips voice platform: an embedded spoken language understanding system for private-by-design voice interfaces,” *CoRR*, vol. abs/1805.10190, 2018.
- [31] F. A. Rodrigues, T. K. D. Peron, P. Ji, and J. Kurths, “The kuramoto model in complex networks,” *Physics Reports*, vol. 610, pp. 1–98, 2016, the Kuramoto model in complex networks.
- [32] T. Lencioni, I. Carpinella, M. Rabuffetti, A. Marzegan, and M. Ferrarin, “Human kinematic, kinetic and emg data during different walking and stair ascending and descending tasks,” *Scientific data*, vol. 6, no. 1, Dec. 2019.
- [33] S. Nuzik, R. Lamb, A. VanSant, and S. Hirt, “Sit-to-Stand Movement Pattern: A Kinematic Study,” *Physical Therapy*, vol. 66, no. 11, pp. 1708–1713, 11 1986.
- [34] R. Socher, A. Perelygin, J. Wu, J. Chuang, C. D. Manning, A. Y. Ng, and C. Potts, “Recursive deep models for semantic compositionality over a sentiment treebank,” in *Proceedings of the 2013 conference on empirical methods in natural language processing*, 2013, pp. 1631–1642.
- [35] A. Wang, A. Singh, J. Michael, F. Hill, O. Levy, and S. R. Bowman, “Glue: A multi-task benchmark and analysis platform for natural language understanding,” 2018. [Online]. Available: <https://arxiv.org/abs/1804.07461>
- [36] X. Liu, P. He, W. Chen, and J. Gao, “Multi-task deep neural networks for natural language understanding,” 2019. [Online]. Available: <https://arxiv.org/abs/1901.11504>